

ELECTRON, PROTON, AND ALPHA MONITOR ON THE ADVANCED COMPOSITION EXPLORER SPACECRAFT

R. E. GOLD, S. M. KRIMIGIS, S. E. HAWKINS, III, D. K. HAGGERTY, D. A. LOHR
and E. FIORE

The Johns Hopkins University Applied Physics Laboratory, Laurel, MD 20732-6099, U.S.A.

T. P. ARMSTRONG and G. HOLLAND

University of Kansas, U.S.A.

L. J. LANZEROTTI

Bell Labs, Lucent Technology, U.S.A.

Abstract. The Electron, Proton, and Alpha Monitor (EPAM) is designed to make measurements of ions and electrons over a broad range of energy and intensity. Through five separate solid-state detector telescopes oriented so as to provide nearly full coverage of the unit-sphere, EPAM can uniquely distinguish ions ($E_i \gtrsim 50$ keV) and electrons ($E_e \gtrsim 40$ keV) providing the context for the measurements of the high sensitivity instruments on ACE. Using a $\Delta E \times E$ telescope, the instrument can determine ion elemental abundances ($E \gtrsim 0.5$ MeV nucl^{-1}). The large angular coverage and high time resolution will serve to alert the other instruments on ACE of interesting anisotropic events. The experiment is controlled by a microprocessor-based data system, and the entire instrument has been reconfigured from the HI-SCALE instrument on the *Ulysses* spacecraft. Inflight calibration is achieved using a variety of radioactive sources mounted on the reclosable telescope covers. Besides the coarse (8 channel) ion and (4 channel) electron energy spectra, the instrument is also capable of providing energy spectra with 32 logarithmically spaced channels using a pulse-height-analyzer. The instrument, along with its mounting bracket and radiators weighs 11.8 kg and uses about 4.0 W of power. To demonstrate some of the capabilities of the instrument, some initial performance data are included from a solar energetic particle event in November 1997.

1. Science Objectives

The Electron, Proton, and Alpha Monitor (EPAM) instrument on the ACE spacecraft is designed to measure a broad range of energetic particles over nearly the full unit-sphere at high time resolution. Such measurements of ions and electrons in the range of a few tens of keV to several MeV are essential to understand the dynamics of solar flares, co-rotating interaction regions (CIRs), interplanetary shock acceleration, and upstream terrestrial events.

The primary objective of EPAM is to support the high sensitivity instruments on ACE. These are the Cosmic Ray Isotope Spectrometer (CRIS), the Solar Energetic Particle Ionic Charge Analyzer (SEPICA), the Solar Isotope Spectrometer (SIS), the Solar Wind Ion Mass Spectrometer (SWIMS), the Solar Wind Ion Composition Spectrometer (SWICS), and the Ultra Low Energy Isotope Spectrometer



(ULEIS). As a monitor instrument EPAM will provide the context for the measurements made by the high sensitivity instruments. The large dynamic range of EPAM extends from about 50 keV to 5 MeV for ions, and 40 keV to about 350 keV for electrons. To complement its electron and ion measurements, EPAM is also equipped with a Composition Aperture (CA) which unambiguously identifies ion species reported as species group rates and/or individual pulse-height events. The instrument achieves its large spatial coverage through five telescopes oriented at various angles to the spacecraft spin axis. The low-energy particle measurements, obtained at time resolutions between 1.5 and 24 s, and the ability of the instrument to observe particle anisotropies in three dimensions make EPAM an excellent resource to provide the interplanetary context for studies using other instruments on ACE.

EPAM is part of the Real-Time Solar Wind (RTSW) system developed by NASA and NOAA. The instrument provides 24-hr coverage of the space weather environment at ACE. The data products include measurements of the real-time flux levels, energy spectra, and anisotropy of energetic ions.

EPAM has some unique capabilities that enable it to provide significant insights in the understanding of energetic particle acceleration and propagation in the heliosphere. Low-energy solar particles will act as probes of the morphology of coronal and interplanetary field structures as they evolve during the rise in solar activity from the near solar minimum conditions at the launch of ACE, through solar maximum. EPAM is the only instrument on the ACE spacecraft that observes the full unit-sphere distribution of particle fluxes; it is the only instrument that measures electrons; it has the highest time resolution of the energetic particle instruments and it covers a wide range of energies with sufficient dynamic range to handle everything from very small events to the most intense solar flares and interplanetary shock spikes. These capabilities will enable EPAM to contribute to the study of a large variety of ACE mission science objectives.

EPAM will examine the acceleration and propagation of ions and electrons in solar energetic particle events. It covers relativistic energies for electrons and non-relativistic ion energies. EPAM covers more than three decades of ion energy including the crucial energy regime spanning the transition from prompt ion propagation at and above 5 MeV nucl^{-1} down to the slower probes of interplanetary field structures at 50 keV. A 32-channel energy spectrum accumulator in EPAM can follow the velocity dispersion of the outflowing ions.

Interplanetary shock acceleration of low-energy ions and electrons is a prominent feature of particle fluxes in the energy range from 50 keV to a few MeV. With its three-dimensional coverage, EPAM can measure the true flow patterns of particles accelerated near shocks. CIRs are also important accelerators of ions, primarily at radial distances beyond 1 AU. The structure and dynamics of particle acceleration at CIRs can be examined in three dimensions by EPAM as these particles flow back into the inner heliosphere. The nearly full unit-sphere coverage of EPAM is important for separating the apparently similar anisotropies observed

resulting from particle flows or cross-field gradients in particle fluxes when they are observed in only two dimensions.

En route from the Earth to the L_1 libration point, ACE observed many bursts of outflowing magnetospheric particles. These bursts, which have been examined both at Jupiter and at Earth, contain many details of particle acceleration and the propagation of the particles upstream to ACE. EPAM will examine the rapid time variations, strong three-dimensional anisotropies and the composition of upstream bursts.

2. Instrument

EPAM is designed to make *in situ* measurements of ions and electrons in interplanetary space. The instrument was adapted from the flight-spare unit of the HI-SCALE instrument aboard the *Ulysses* spacecraft. HI-SCALE was built by the Johns Hopkins University Applied Physics Laboratory with Dr Louis J. Lanzerotti of Lucent Technologies as Principal Investigator; detailed descriptions of HI-SCALE may be found elsewhere (Lanzerotti et al., 1983, 1992, 1993). Although HI-SCALE and EPAM are identical in design and functionality, the mechanical layout of the detectors making up the HI-SCALE instrument was designed for an unimpeded field-of-view when mounted on the corner of the box-like structure of *Ulysses*. In order to provide EPAM with an unimpeded field-of-view on the irregular octagon structure of ACE, the two telescope assemblies were moved to a mounting fixture, elevated above the spacecraft top deck and located between two solar arrays (see Chiu et al., this issue). An interface box was added to the EPAM electronics to convert the control signals sent to and received from the ACE spacecraft, in order to use the *Ulysses* spacecraft interface.

EPAM measures energetic particles in the energy range from about 50 keV to 5 MeV. Its configuration consists of five solid-state detector systems on two stub telescopes, referred to as the 2A and 2B assemblies. The telescopes are mounted on a support bracket, which also mounts and encloses the instrument electronics box. The EPAM instrument alone weighs approximately 5.64 kg and the instrument along with its mounting bracket weighs 11.8 kg. Although survival heaters are present, the nominal instrument temperature is well above the thermostatic set point of these heaters, and so they will not cycle on. EPAM consumes about 4.0 W of power during normal operations. Table I summarizes the characteristics of EPAM.

Each stub telescope supports a Low-Energy Magnetic Spectrometer (LEMS) to measure ions, and a Low-Energy Foil Spectrometer (LEFS) that measures both ions and electrons. These two detector systems together form a LEMS/LEFS pair which is identical in design on each stub-arm telescope. The two LEMS sensors are oriented 30° and 120° from the spin axis and are identified as LEMS30 and LEMS120. The LEFS are pointed 60° and 150° from the spacecraft spin axis and are known as the LEFS60 and LEFS150 telescopes. The last detector system

TABLE I
ACE/EPAM instrument characteristics

Mass	instrument	5.64 kg
	bracket	6.13 kg
Power		4.0 W
EPAM data rate		168 bits/s, continuous
Thermal control		passive
Spatial coverage		5 apertures, \approx full unit sphere
Time resolution		1.5–6 s
Energetic particles	electrons	40– \approx 350 keV
	ions	46–4800 keV
	species groups	H, He, CNO, Fe
Geometric factors	LEMS	0.428 cm ² sr
	LEFS	0.397 cm ² sr
	CA	0.103 cm ² sr

measures ion composition, and is referred to as the Composition Aperture (CA). Its look-direction is oriented 60° from the spacecraft spin-axis and so is known as the CA60 telescope.

The two LEMS telescopes and the CA60 telescope have covers that may be commanded closed by heating bi-metallic springs attached to each cover. Radioactive sources mounted in the covers provide inflight calibration of the LEMS and CA detector systems. A photograph of the instrument is shown in Figure 1, with labels indicating the five detector assemblies.

ACE is a spin-stabilized spacecraft which rotates about an axis directed within 20° of the Sun at a rate of about 5 revolutions per minute and hence a spin period of 12 s. As the spacecraft spins, these five telescopes sweep out swaths of space, providing nearly full three-dimensional coverage for measuring ion anisotropies and approximately 40% coverage for electron anisotropies. As the spacecraft spins, the instrument electronics sample the detectors such that the swath of space swept out by each telescope is divided into nearly equally spaced sectors.

Figure 2 shows the EPAM look directions and the approximate sector definitions, projected onto the unit sphere, as well as a cylindrical projection of these look directions for the five sensor heads. The abscissa denotes the clock angle in degrees from the spacecraft x -axis. The ordinate gives the polar angle from ACE's spin vector. In the case of the detector pair, LEMS30/LEFS150, four sectors are used, each 90° wide. These sectors are referred to by the upper case letters A to D for LEMS30 and the numbers 1 to 4 for the LEFS150. The LEMS120/LEFS60 detector pair is divided into eight sectors, each 45°. These sectors are denoted in the figure by the numbers 1 through 8 for LEMS120, and the letters a to h for the

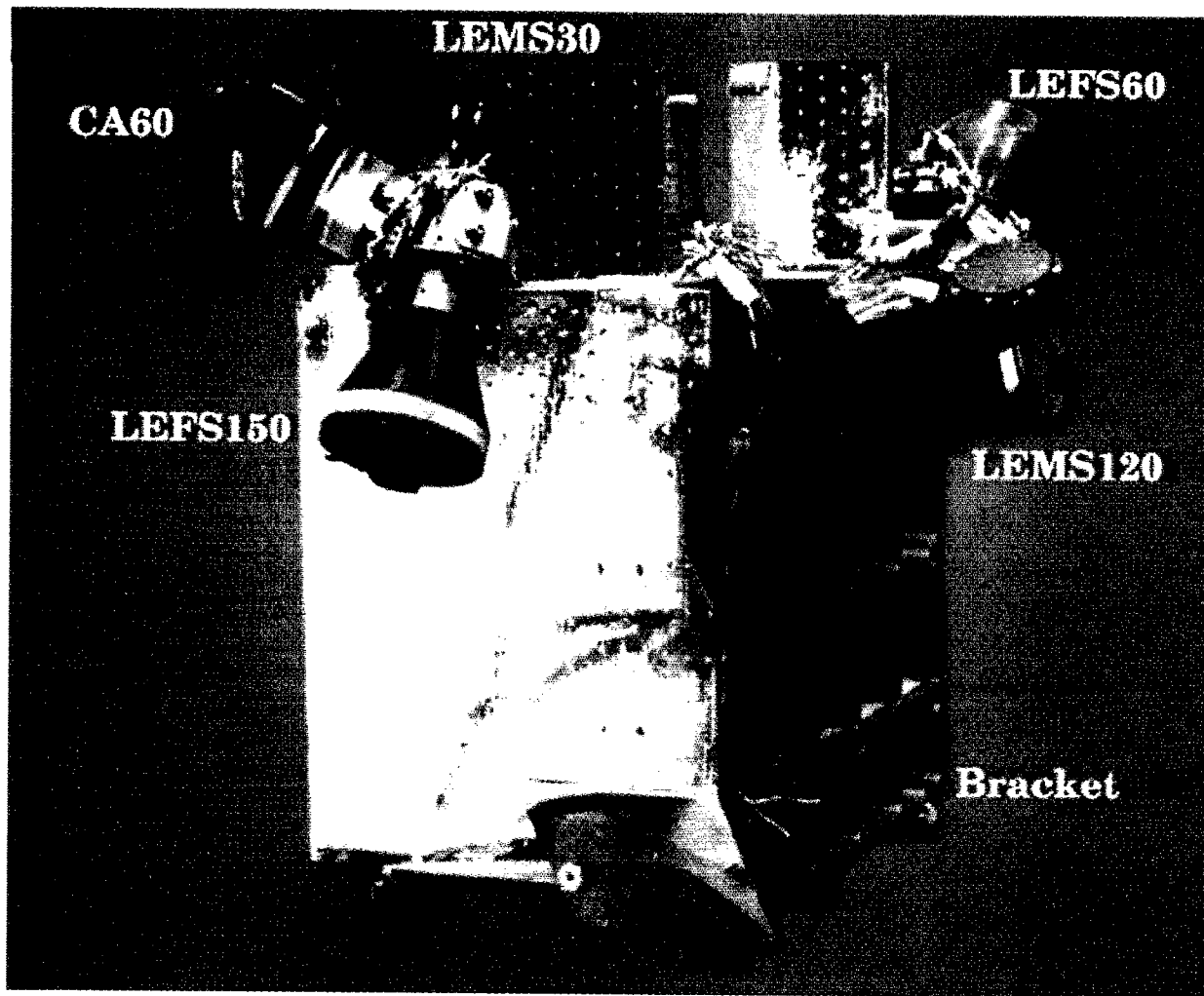


Figure 1. The EPAM instrument on ACE. The five detector orientations on the two stub-arm telescopes are designed to provide nearly full coverage of the unit sphere as the spacecraft spins. The LEMS and the CA detectors have reclosable covers and are used for inflight calibrations.

LEFS60 system. The CA60 telescope also is sampled in 8 sectors. From this figure, it is clear that EPAM covers most of the unit-sphere, with considerable overlap in spatial coverage.

2.1. DETECTOR SYSTEMS

A schematic view of the EPAM 2A and 2B stub-arm telescope configurations is shown in Figure 3. The EPAM 2A configuration shows the LEMS120/LEFS60 telescope pair. The 2B configuration shows the LEMS30/LEFS150 pair, as well as the CA60 telescope and its detectors (discussed below). The two LEFS detectors have a full-cone angle of 53° and a geometric factor of $0.397 \text{ cm}^2 \text{ sr}$. The two LEMS detectors have a full-cone angle of 51° and a geometric factor of $0.428 \text{ cm}^2 \text{ sr}$. The CA has a reduced geometric factor of $0.103 \text{ cm}^2 \text{ sr}$ and a full-cone angle of 45° .

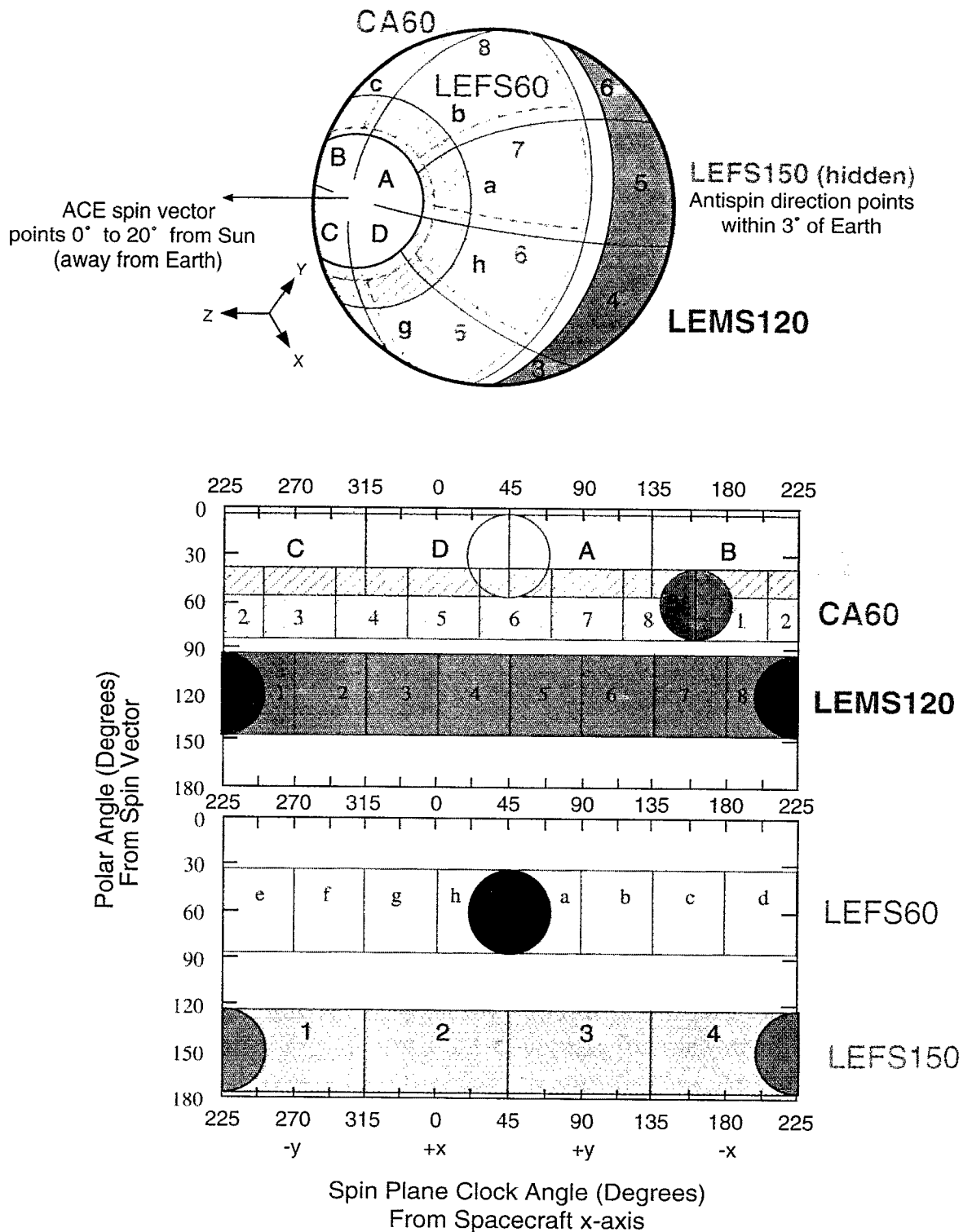


Figure 2. The five EPAM detector assemblies are shown in a cylindrical projection. The energy channels for each of the telescopes are abbreviated for the electrons as E (LEFS150) and E' (LEFS60). The ion channels are denoted by P (LEMS30) and P' (LEMS120), and the composition channels by W (CA60). The abscissa shows the clock angle measured from the spacecraft's x -axis. Depending on the detector, either 4 or 8 sectors divide a spin into approximately equally spaced regions. The ordinate shows the polar angle measured from the spin vector of ACE.

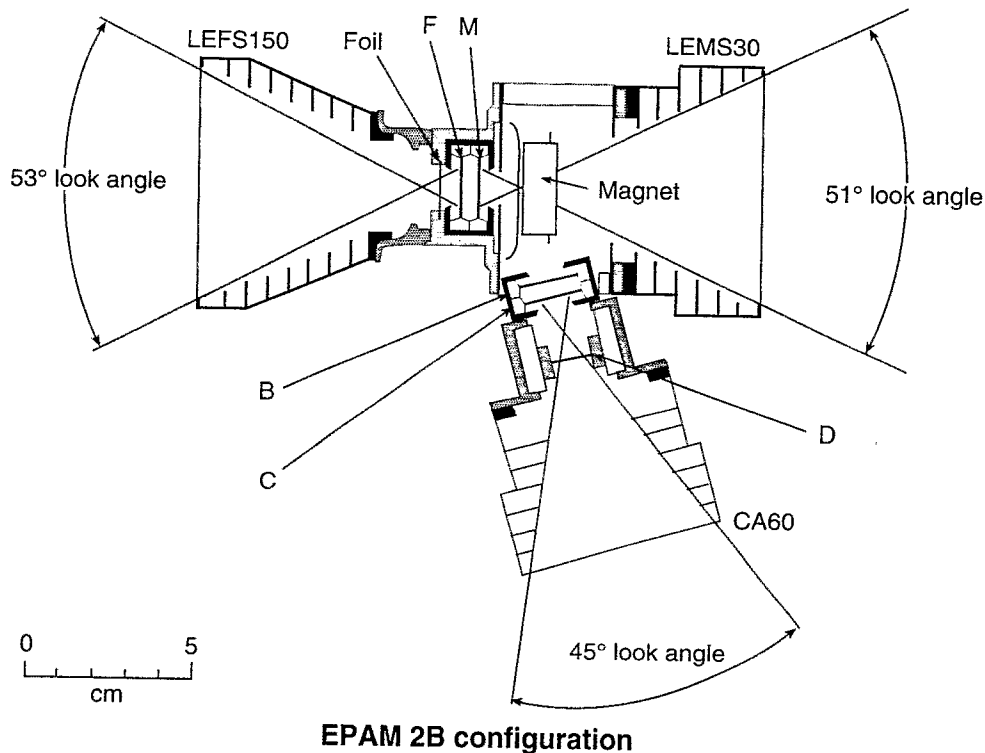
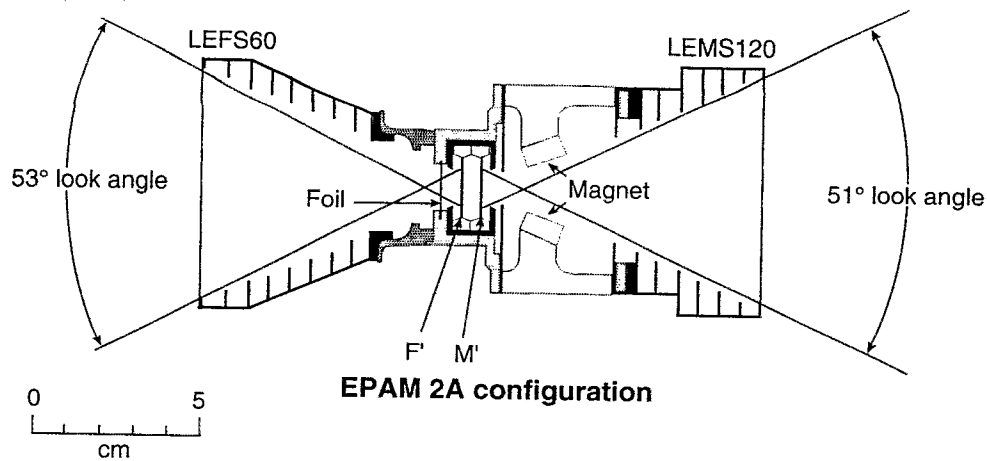


Figure 3. Schematic outline of the EPAM instrument's detector assemblies. The detectors are identified by the letters M , F , M' , F' , B , C and are totally depleted surface barrier Si detectors, each approximately $200\ \mu\text{m}$ thick. The D detector is $4.8\ \mu\text{m}$ thick.

2.1.1. LEMS/LEFS

The LEFS60 and LEFS150 telescopes measure electrons with energies less than about 350 keV. An aluminized Parylene foil, nominally $0.35\ \text{mg cm}^{-2}$ thick, is used to absorb ions with energies below approximately 350 keV, while allowing electrons with energies above about 35 keV to pass through to the solid-state detector. The detector assemblies are referred to as F and F' for the LEFS150 and LEFS60 telescopes, respectively.

The two LEMS telescopes measure ions and these detectors are referred to as M for the LEMS30 telescope, and M' for the LEMS120 telescope. A rare-earth magnet in front of each of the two LEMS detectors, M and M' , sweeps out any electrons

TABLE II
Low-energy magnetic spectrometer detector systems

LEMS30			LEMS120		
Energy channel	Logic	Passband (MeV)	Energy Channel	Logic	Passband (MeV)
<i>P</i> 1	$M1\overline{M2F}$	0.046–0.067	<i>P'</i> 1	$M'1\overline{M'2F'}$	0.047–0.068
<i>P</i> 2	$M2\overline{M3F}$	0.067–0.115	<i>P'</i> 2	$M'2\overline{M'3F'}$	0.068–0.115
<i>P</i> 3	$M3\overline{M4F}$	0.115–0.193	<i>P'</i> 3	$M'3\overline{M'4F'}$	0.115–0.195
<i>P</i> 4	$M4\overline{M5F}$	0.193–0.315	<i>P'</i> 4	$M'4\overline{M'5F'}$	0.195–0.321
<i>P</i> 5	$M5\overline{M6F}$	0.315–0.580	<i>P'</i> 5	$M'5\overline{M'6F'}$	0.310–0.580
<i>P</i> 6	$M6\overline{M7F}$	0.580–1.060	<i>P'</i> 6	$M'6\overline{M'7F'}$	0.587–1.060
<i>P</i> 7	$M7\overline{M8F}$	1.060–1.880	<i>P'</i> 7	$M'7\overline{M'8F'}$	1.060–1.900
<i>P</i> 8	$M8\overline{F}$	1.880–4.700	<i>P'</i> 8	$M'8\overline{F'}$	1.900–4.800

with energy below about 500 keV. In the LEMS30 telescope, these electrons are measured in the *B* detector which is located at the back of the CA60 telescope assembly (described in Section 2.1.3). The *B* detector is also the anti-coincidence detector of the CA. Because the *B* detector measures deflected electrons, it is a pure electron detector and is not generally susceptible to ion contamination.

Each of the four detectors (*M*, *F*, *M'*, *F'*) used in the LEMS/LEFS telescopes is a totally depleted, solid-state, silicon surface barrier detector with a total thickness of approximately 200 μm . The penetrating particle creates electron-hole pairs in the detector, the number of which is related to the incident kinetic energy of the particle. Provided the detector stops the particle, its total energy can be inferred. Completely analogous to LEMS30, the LEMS120 telescope uses the *M'* detector, and the differential flux is measured in eight rate channels, *P'*1 through *P'*8. Table II gives the energy channel name, the logic equation implemented by the instrument electronics, and the energy passbands for the two LEMS detector systems. The overall EPAM block diagram (adapted from Lanzerotti et al., 1992) is shown in Figure 4.

The LEFS150 telescope uses detector *F* to measure rate and energy and detector *M* serves as its anti-coincidence detector. The differential flux of the particles is determined from the total electron energy in three energy channels, referred to as *E*1 to *E*3. Four additional energy channels are used to measure ions above about 400 keV which penetrate the foil and stop in the *F* detector. These channels are referred to as *FP*4 to *FP*7 where the notation '*FP*' is used to emphasize that these particles are foil protons (ions). The energy of these ions may be inferred by adding the energy loss through the foil to the electronic energy channel passbands. Pure electrons are measured in the *B* detector of the CA60 telescope, described below. Table III gives the energy channel name, the logic equation implemented

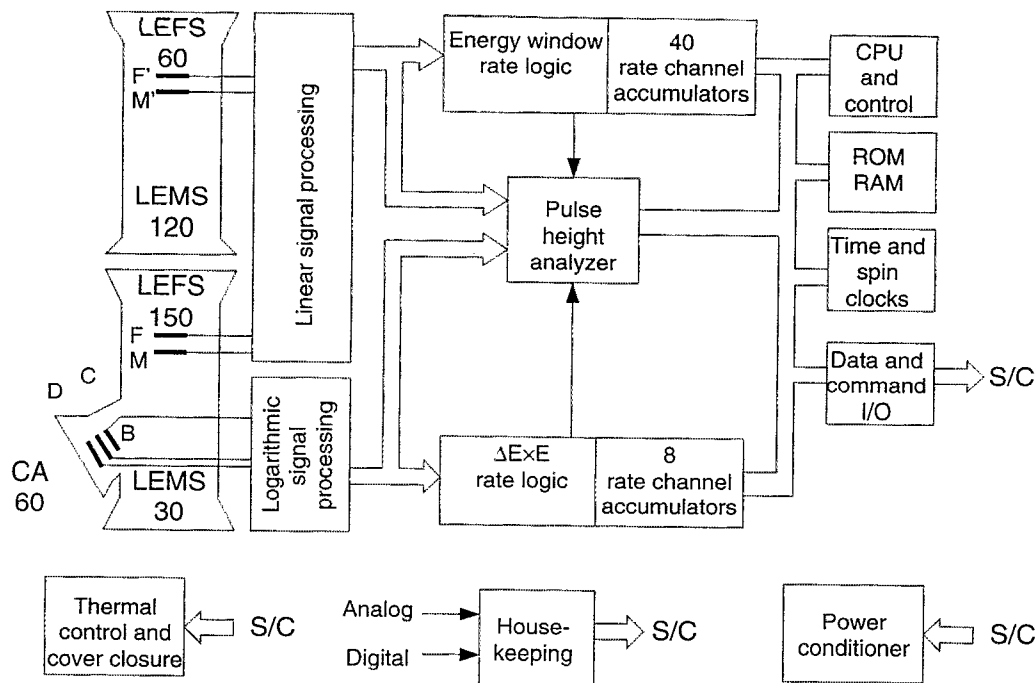


Figure 4. Block diagram of the EPAM instrument electronics.

TABLE III
Low Energy Foil Spectrometer detector systems

LEFS150			LEFS60		
Energy channel	Logic	Passband (MeV)	Energy Channel	Logic	Passband (MeV)
$E1$	$F1\overline{F2}M$	0.044–0.058	$E'1$	$F'1\overline{F'2}M'$	0.045–0.062
$E2$	$F2\overline{F3}M$	0.058–0.104	$E'2$	$F'2\overline{F'3}M'$	0.062–0.102
$E3$	$F3\overline{F4}M$	0.104–0.180	$E'3$	$F'3\overline{F'4}M'$	0.102–0.175
$FP4$	$FP4\overline{F5}M$	0.463–0.568	$FP'4$	$F'4\overline{F'5}M'$	0.463–0.568
$FP5$	$F5\overline{F6}M$	0.568–0.796	$FP'5$	$F'5\overline{F'6}M'$	0.568–0.795
$FP6$	$F6\overline{F7}M$	0.796–1.114	$FP'6$	$F'6\overline{F'7}M'$	0.795–1.193
$FP7$	$F7\overline{M}$	1.114–4.924	$FP'7$	$F'7\overline{M'}$	1.193–4.924

by the instrument electronics, and the energy passbands for the two LEFS detector systems. The LEFS60 telescope uses the same detection scheme with the F' detector to measure rate and energy with M' used in anti-coincidence. Energetic electrons above about 350 keV will pass through the foil and the 200 μm thick detector $F(F')$, and will be detected by the anti-coincidence circuit when they are detected in the $M(M')$ detector.

2.1.2. *MF Spectrum Accumulator*

The MF Spectrum Accumulator, or MFSA, provides much higher energy resolution for the LEMS and LEFS detector systems than is available from the rate channels. This feature of the EPAM electronics produces a 32-point logarithmically spaced energy spectrum, accumulated from each of the LEMS/LEFS detectors. These data are processed according to a schedule which rotates through each sector of the detectors M , F , M' , F' .

The MFSA samples the same analog signal as the rate channels and converts it to a logarithmic signal, then digitizes it to 8 bits rather than processing the analog signal with discriminators and accumulators, as is done with the rate channels. The MFSA digitization is identified in Figure 4 as the central block labeled 'Pulse-height analyzer.' At the time the instrument was designed, space qualified 8-bit analog-to-digital converters required about $30 \mu\text{s}$ to complete one conversion. This slow rate could not keep up with the analog portion of the instrument, hence only a subset of events could be processed.

The MFSA accumulation scheme is summarized in Table IV. Each row corresponds to a schedule in the MFSA accumulation. The MFSA data system consists of a bank of four memories which are multiplexed to store the 32-bin, 8-bit spectra, on a per sector basis. These four memory banks are denoted by the Roman numerals I–IV in Table IV. The LEMS30 and LEFS150 telescopes each have four sectors, and therefore accumulate a spectrum from detectors M , F for each sector in a single schedule of 128 s. The eight sectored detectors (M' , F') require two schedules to accumulate a 32-bin spectrum for each sector. The sectors in Table IV are denoted by the letters A–D for the four sectored telescopes, and the numbers 1–8 for the eight sectored ones. An entire collection cycle requires 1024 s.

2.1.3. *Composition Aperture*

The CA telescope is capable of determining ion composition using a $\Delta E \times E$ detection scheme. Although the principal responsibility of EPAM is to monitor electrons, protons, and alphas, the CA provides an unambiguous determination of ion composition, unlike the LEMS detectors. The CA60 telescope is comprised of three solid-state detectors (cf., Figure 3): a thin, $4.8 \mu\text{m}$ epitaxial silicon detector referred to as the D detector, and two thick ($\sim 200 \mu\text{m}$) totally depleted surface barrier silicon detectors known as C and B . The B detector, as mentioned previously, measures deflected electrons from the LEMS30 head, but also acts as the anti-coincidence detector for the CA.

The CA system uses log amplifiers to extend the dynamic range of the detector. These amplifiers are extremely temperature sensitive, and therefore are thermally regulated with heaters to maintain calibration. The logic used in the CA depends on slanted discriminators to define each species group. The eight CA rate channels, denoted by the symbols W1 to W8, count all particles in a given energy nucl^{-1} range. Multiple species may therefore be associated with a single CA rate channel. As a result, a species group is identified by the dominant species in that group.

TABLE IV

Schedule for the accumulation of the 32 point spectra produced by the MFSA for each detector and sector of the LEMS and LEFS systems. Each schedule (row) requires 128 s to process and each sector's spectrum is stored in one of four 32 byte memory banks (I-IV).

Schedule	Detector	Sector in memory bank			
		I	II	III	IV
0	<i>M</i>	A	B	C	D
1	<i>F'</i>	a	c	e	g
2	<i>M'</i>	1	3	5	7
3	<i>F'</i>	b	d	f	h
4	<i>M'</i>	2	4	6	8
5	<i>F'</i>	a	c	e	g
6	<i>F</i>	1	2	3	4
7	<i>F'</i>	b	d	f	h

Table V lists the detailed information for each group. Defined for each energy channel *W* is the count rate logic, the energy passbands of the dominant species in each species group, the identifier of the group, and the atomic number response. An example of the multiplicity of species for a given species group is given by the O-species group. This group is defined by the rate channels denoted W5 and W6 and is dominated by oxygen; however, there is also a significant contribution from carbon and nitrogen. This group is therefore also identified as the CNO group. Similarly, the Fe-group is made up of all species with $10 \leq Z \leq 28$, but here iron is the dominant species. The energy passbands for the magnetically deflected electrons from the LEMS30 are also shown in Table V. Note that the lowest energy channel in detector *B* has a selectable low threshold level.

Like the MFSA system described above, timing and downlink constraints make it impossible to process every event from the two detectors *D* and *C* using an 8-bit analog-to-digital converter. Therefore, an adaptive priority scheme was designed into the instrument to selectively process PHA events. In this scheme, the less abundant species such as Fe and O are preferentially selected over the dominant constituents of H and He. The method makes use of the fast but coarse characterization of the rate channels W1 to W8. The logarithmic analog signal from the detector is digitized to 8 bits provided that it falls within the appropriate rate channel.

The adaptive priority scheme, shown in Table VI, determines what species group (cf., Table V) to analyze, based on the last species group analyzed. This

TABLE V
Composition aperture detector system

Energy channel	Logic	Passband (MeV nucl ⁻¹)	Species group*	Z
W1	$C1D1\overline{C2D2B}$	0.521-1.048	H	1
W2	$C2D1\overline{D4D2S1B}$	1.048-1.734	H	1
W3	$C1(D2 + S1)\overline{C3D3B}$	0.389-1.278	He	2
W4	$C3D1S1\overline{C4D3B}$	1.278-6.984	He	2
W5	$C2D3\overline{C4D4B}$	0.546-1.831	O	6-9
W6	$C4D2S2\overline{D4S3B}$	1.831-19.107	O	6-9
W7	$C2D4\overline{C4B}$	0.298-0.955	Fe	10-28
W8	$C4D3S3\overline{B}$	0.955-92.663	Fe	10-28
		(keV)		
DE1	$B1a\overline{B2C}$	38-53	electrons	
	$B1b\overline{B2C}$	48-53	electrons	
DE2	$B2\overline{B3C}$	53-103	electrons	
DE3	$B3\overline{B4C}$	103-175	electrons	
DE4	$B4\overline{B5C}$	175-315	electrons	

*These species and passbands correspond to the dominant species in each group. The reader is referred to Table III. of Lanzerotti et al. (1993) for the passbands of additional species.

TABLE VI

Adaptive priority scheme used in the CA system.
Note that each species in the table refers to a species group defined in Table V.

		Species group of previous event			
		H	He	O	Fe
Priority for current event	Highest	Fe	H	He	O
		O	Fe	Fe	Fe
		He	O	O	He
	Lowest	H	He	H	H

is done for each of the eight sectors of the CA. For example, if in sector 3, the last species group analyzed was Fe, then the priority for the current event would be taken from the last column of Table VI. Thus, if an oxygen event were available, it would get processed, otherwise, the instrument would process Fe, He, or H, in that order, based on the availability of each. In this way, the instrument should analyze a larger number of the rare species.

Two PHA events are downlinked for each ~ 1.5 s sector for an average rate of about 1.3 events per second. Of these two events, it is the lower priority event that is used to drive the adaptive priority scheme for the same sector on the next spacecraft rotation.

3. Calibration

A ground-based calibration was performed on the EPAM instrument prior to launch. Such a characterization of the instrument is essential in order to understanding the inflight measurements made by EPAM. Such calibration data include determination of the electronic thresholds and verification of these thresholds using calibrated pulsers. The ground-based calibration also included characterization of the instrument response to accelerated beams of ions and electrons in order to verify the energy channel thresholds. EPAM also has the capability to perform inflight calibrations.

3.1. PREFLIGHT CALIBRATION

The basic instrument functions and electronic thresholds of EPAM have been exercised and measured both as the flight spare instrument of HI-SCALE, and after the instrument was reconfigured as EPAM. The LEMS and LEFS telescopes of the EPAM instrument were characterized using the two particle accelerators at the NASA Goddard Space Flight Center. These accelerators were able to stimulate a limited number of EPAM's energy channels and verify the channel thresholds.

An electrostatic accelerator was used to calibrate the lower energy channel thresholds of the LEMS and LEFS telescopes using protons and electrons, respectively. These accelerated particle beams ranged in energy from 32 to 114 keV for protons and 40 to 117 keV for the electrons. The higher energy channels of the LEMS telescopes were stimulated by protons and helium ions that were accelerated by a Van de Graaff generator. The proton beam was varied in energy from 0.391 to 1.492 MeV and the helium ions ranged from 1.500 to 1.608 MeV.

3.2. INFLIGHT CALIBRATION

EPAM was designed with inflight calibration capabilities that provide discrete high-energy helium and electron emissions to verify proper instrument operation. Calibration sources are mounted inside the covers of the CA and LEMS telescopes.

TABLE VII
EPAM inflight calibration sources

Telescope	Source	Strength (μCi)	Particle Energy, Type	X-ray (keV)	Half-life (yrs)
CA60	^{244}Cm	1.0	5.81 MeV, α		18.11
	^{148}Gd	0.16	3.18 MeV, α		75
LEMS120	^{241}Am	1.0	5.49 MeV, α	59.5	432.2
LEMS30	^{241}Am	1.0	5.49 MeV, α	59.5	432.2
	^{133}Ba	1.0	45 keV, β	31, 80, 302, 356	10.5

By commanding heaters to turn on, the bi-metallic springs attached to each cover of the LEMS and CA telescopes will slowly close, permitting an inflight calibration to be performed and the instrument's response measured.

Each LEMS cover contains a $1.0 \mu\text{Ci}$ ^{241}Am source which emits α particles at 5.486 MeV which will be observed in the highest LEMS energy channel. The source also emits ~ 60 keV X-rays which are observable in the lowest LEMS energy channel. The LEMS30 telescope cover also contains a $1.0 \mu\text{Ci}$ ^{133}Ba calibration source. The barium source provides a range of energetic electrons that enter the LEMS30 telescope and are magnetically deflected into the *B* detector of the CA. The CA60 telescope cover contains a dual $1.0 \mu\text{Ci}$ ^{244}Cm and $0.16 \mu\text{Ci}$ ^{148}Gd calibration source that provides 5.8 MeV and 3.183 MeV alpha particles. These peaks are observed in the W3 and W4 channels. Table VII summarizes the radioactive sources for each telescope, the particle type and energy, and selected X-ray emissions.

4. Inflight Performance

The ACE spacecraft was launched from Cape Canaveral on 25 August 1997 and two days later EPAM was turned on. An initial 75-min inflight calibration test was performed prior to commanding the pyrotechnic devices to fire, releasing the covers on the LEMS and CA telescopes, containing the radioactive sources. Since that time, EPAM has performed well with immediate observations of upstream magnetospheric events, solar events, and other interplanetary phenomena.

4.1. IONS AND ELECTRONS

An example of the wide range of observations possible with EPAM is shown in Figure 5. Six selected channels from the instrument are plotted for the twelve-day

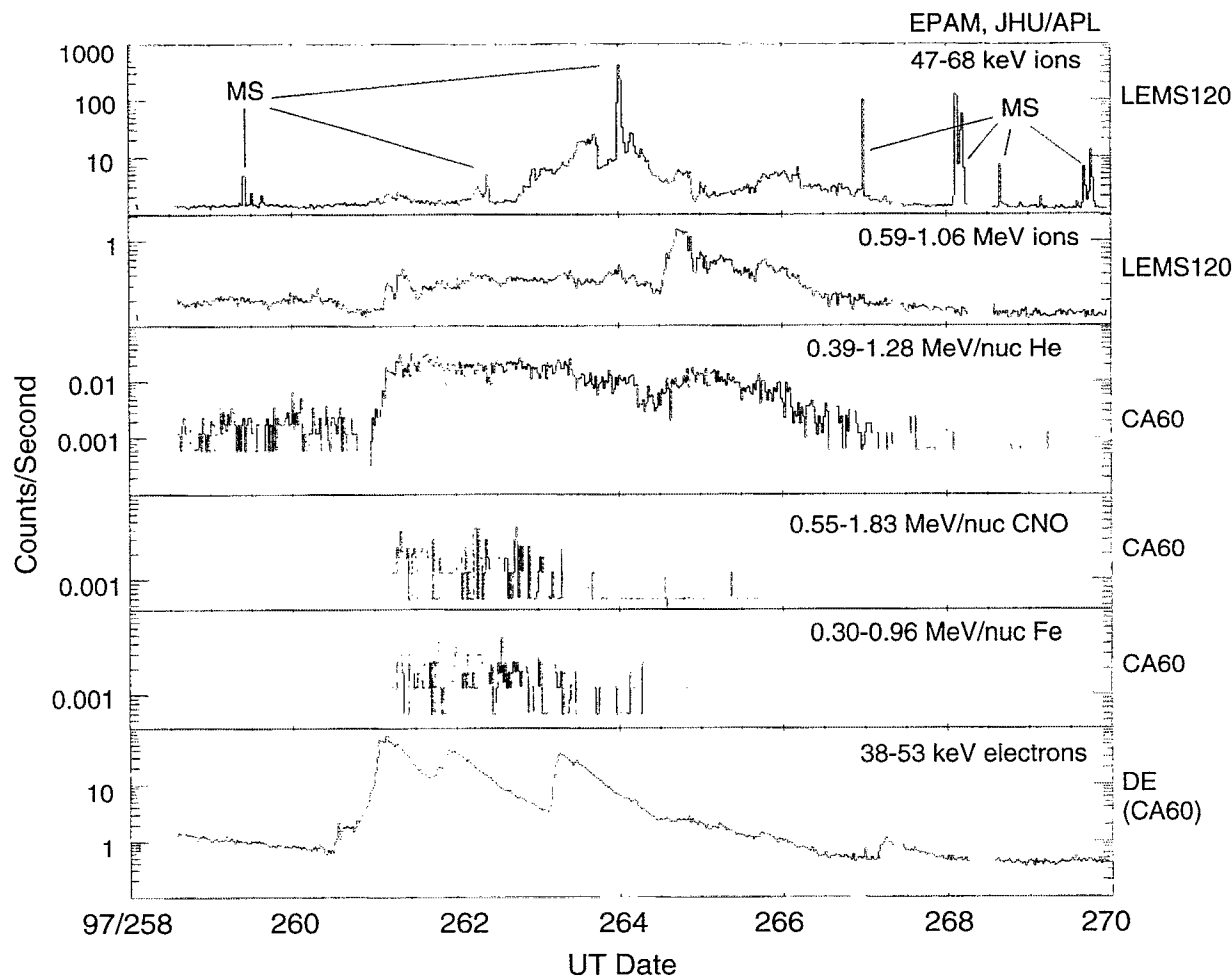


Figure 5. Selected channels from EPAM during a 12 day interval about a month after the instrument was turned on.

period from 15–27 September 1997. The top curve shows LEMS120 response to the 47–68 keV ions. The LEMS120 telescope, with its slightly oblique view of the terrestrial magnetosphere, resolves numerous upstream magnetospheric events, labeled MS, during this 12 day period. Nearly one hundred upstream, magnetospheric events were observed in the first 30 days of the mission. The second panel shows LEMS120 response to ions in the 0.587–1.060 MeV energy range. The magnetospheric events shown for this time interval have relatively soft spectra and do not extend beyond 500 keV, thus a very different profile is seen in the higher energy ions. The third, fourth, and fifth panels in Figure 5 show the instrument's capabilities at measuring and differentiating the composition of the observed ions at higher energies.

The CA60 telescope samples ions at 60° from the spin axis, and since it does not point back to the magnetosphere, it observed a very different ion profile than was observed at 120° from the spin axis. The third panel shows a steep rise on day 261 in the 0.389–1.278 MeV nucl^{-1} helium flux. The intensity of the helium ions remains enhanced for a number of days before decaying away after day 266. The fourth and fifth panels show responses to 0.546–1.831 MeV nucl^{-1} CNO group ions

and 0.298–0.955 MeV nucl^{-1} Fe group ions, respectively. The ion composition during the first portion of this small solar event is very rich in He and heavy nuclei with the Fe group ions about as plentiful as the CNO group. The last panel in Figure 5 shows the magnetically deflected electrons, 38–53 keV, from the LEMS30 telescope. The onset of the triple solar electron event is seen in phase with the onset of the helium ions, and the smaller enhancement of the 0.587–1.060 MeV channel of the LEMS120 ions.

Figure 6 shows about four hours of data during a series of upstream magnetospheric events with higher temporal and angular resolution than was shown in Figure 5. The eight curves are the responses to 47–68 keV ions of the eight angular sectors in the LEMS120 cone. The event onset began shortly after 11:00 UT, labeled A, where the count rates rose to about 100 c s^{-1} in all sectors and remained at that intensity for about 10 min. The intensities then jumped to about 1000 c s^{-1} , however, the varying profiles from one sector to the next are indicative of the highly structured nature of some upstream events.

A second event, labeled B, shows a period where count rates in sectors 2, 3, and 4 were very intense, but the opposite looking sectors 7 and 8, showed no significant enhancement. This event illustrates the effectiveness of the angular resolution of the EPAM instrument, and the strong anisotropic behavior characteristic of many upstream events. The third event during this time, labeled C, shows a small but clear temporal difference in the event onset between sector 2, arriving just after the event, and sector 6, arriving just before the event. The time difference between the event onset in these two sectors is about 7 min.

In Figure 7, two anisotropy pie-plots are shown during the events labeled (B) and (D) in Figure 6. The large anisotropy is clearly seen in Figure 7(a) where the ion count rates in sectors 3 and 4 reach nearly 1000 c s^{-1} while virtually no counts above background are observed in sectors 7 and 8. Figure 7(b) shows the nearly isotropic behavior about 1.5 hour later.

A large solar event was observed by EPAM on 6 November 1997 and the instrument's electron, ion, and species composition responses are shown in Figure 8. The top group of curves shows the 38 to 315 keV magnetically deflected electrons (cf., Table V), averaged over a spacecraft spin and a 1-hr time interval. The middle panel shows selected responses to 47 to 1900 keV ions, and the final group shows the CA responses to 0.521–1.048 MeV nucl^{-1} protons, 0.389–1.278 MeV nucl^{-1} He, 0.546–1.831 MeV nucl^{-1} CNO group ions, and 0.298–0.955 MeV nucl^{-1} Fe group ions. The onset of the event is clearly seen from the energetic electrons, while a strong shock spike is seen in the ion responses later in the day.

Figure 9 shows four selected energy spectra from the MF Spectrum Accumulator which has 32 logarithmically spaced channels. Figure 9(a) shows the first spectrum which is a 128-s average of ions observed at 120° from the spin axis, prior to the onset of the first solar event. The second spectrum (b) shows the higher energy ions, $E > 1 \text{ MeV}$, arriving at the spacecraft while the lower energy ions are still at pre-event intensities. The third spectrum (c) shows the enhancement

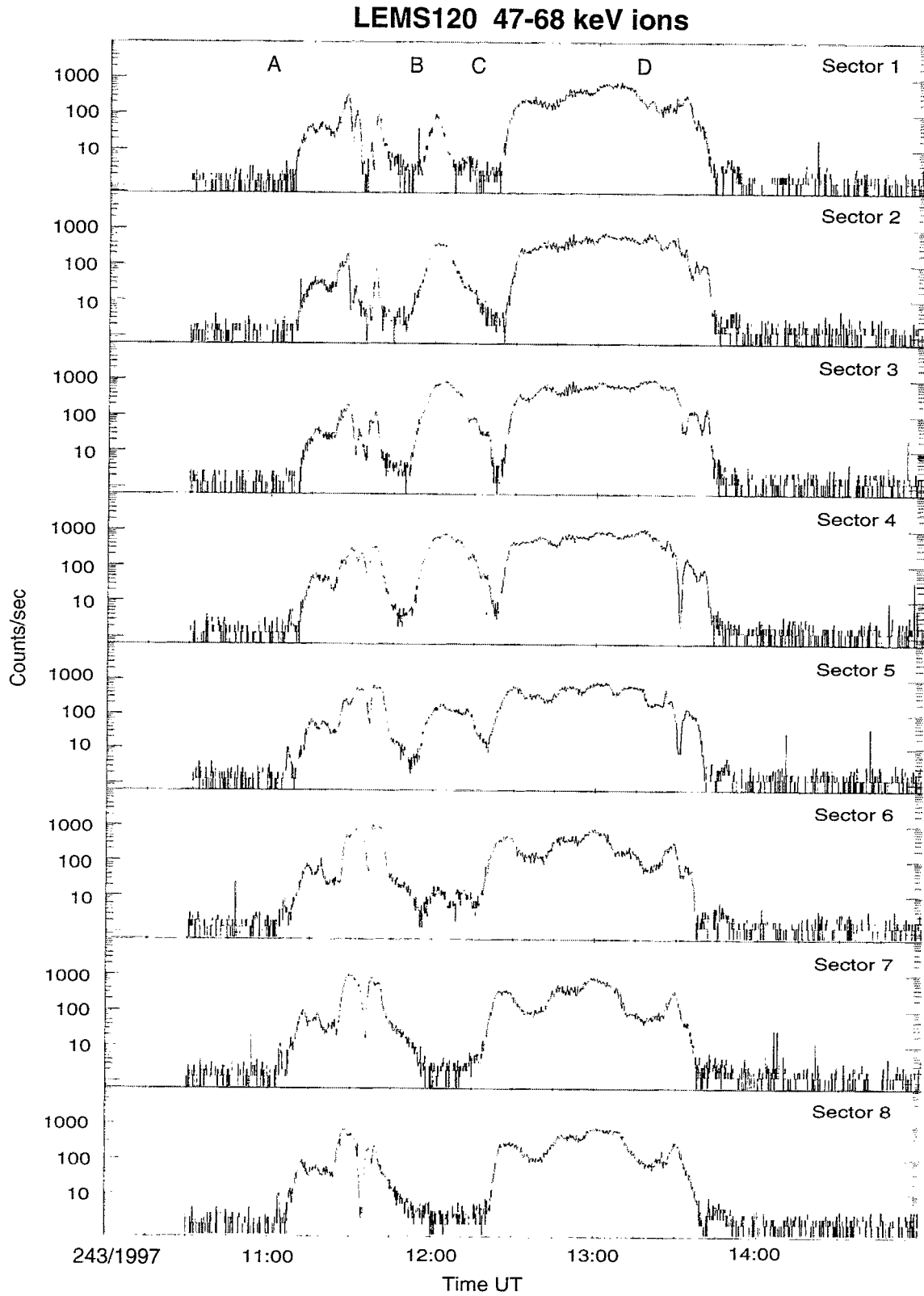


Figure 6. High time resolution rate channel data from day 243 (1 September 1997). All eight sectors of the LEMS120 telescope are shown and depict the high anisotropy of this event.

Lems120 anisotropy

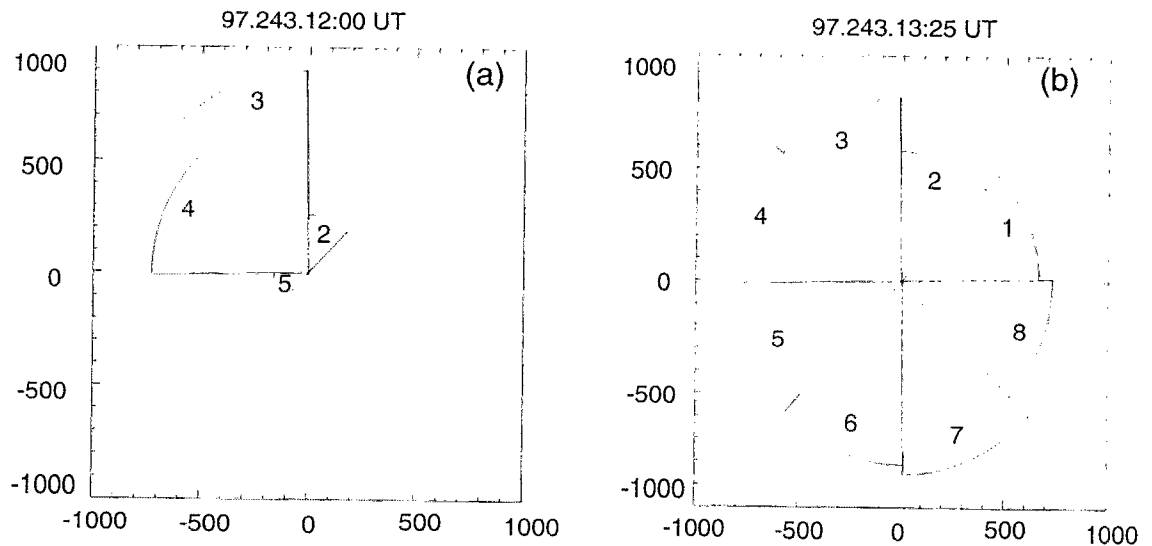


Figure 7. Anisotropy plots from EPAM showing very different distributions for two times on day 243 (1 September 1997). In (a) the strong anisotropy is seen in sectors 3 and 4, measured at 12:00 UT (labeled B in Figure 6), whereas in (b) the nearly isotropic distribution was measured at 13:25 UT (label D in Figure 6).

extending down to low energies. The fourth spectrum (d) shows the ion responses right at the shock spike. The energy dependence of the shock accelerated ions is clearly evident in the EPAM spectrum.

All events in the CA telescope are pulse height analyzed and the two highest priority events in each sector are telemetered to the ground. Figure 10 is a 12-hr accumulation of the pulse height matrix plotted by the energy deposited in detectors C and D for each event. Individual atomic species form clearly defined tracks which show the species resolution of EPAM.

The boundaries labeled W1–W8 show the mapping of the CA species-group rate channels into pulse-height space using the logic equations given in Table V. Within these limits, all particles are counted, independent of the adaptive priority scheme, and these rates are used to normalize the tracks shown in the PHA matrix.

5. Summary

The EPAM instrument provides comprehensive energy, angular, and species coverage with good resolution over a key parameter space in studies of energetic particles in the near Earth interplanetary medium. As such, it serves to highlight the context in which the detailed compositional, isotopic, and charge-state measurements of the principal ACE instruments can be properly assessed and interpreted. Further, several key channels are used to provide real-time information on space weather status (see Zwickl et al., 1998) that is utilized by NOAA and broadcast worldwide to all users. Finally, EPAM serves as an excellent baseline at 1 AU for studies of radial and latitudinal gradients in conjunction with an instrument of

EPAM electron, ion, and species observations

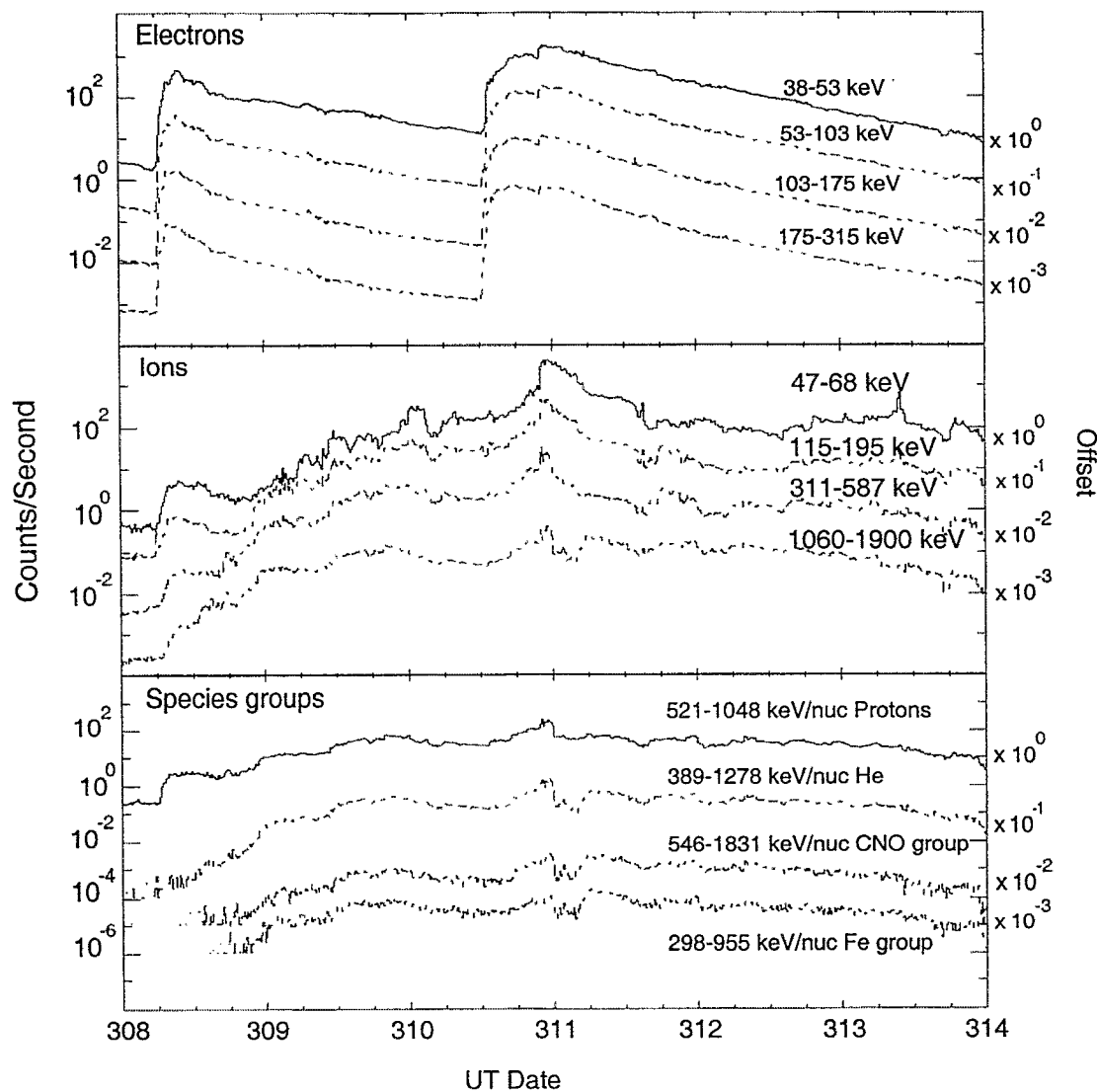


Figure 8. Rate channel data from the EPAM magnetically deflected electrons, LEMS120 ions, and species groups from the CA showing the time progression of the particles resulting from a large solar energetic particle event in November 1997.

identical design on the *Ulysses* spacecraft. The quality of the initial data shown in this paper is such that there is every expectation for a long-term, continuous data stream documenting the onset of the new solar cycle.

Acknowledgements

Although EPAM started from a working *Ulysses* spare instrument, a great deal of effort was required to convert the HI-SCALE spare unit into the final EPAM instrument. We cannot acknowledge all of those who have helped in this effort, however, a few people who worked very long and hard must be recognized. B. E. Tossman served as the project manager, G. B. Andrews was the system engineer during the first half of the EPAM project, T. G. Sholar was the mechanical engineer,

EPAM LEMS 120 MFSA ions

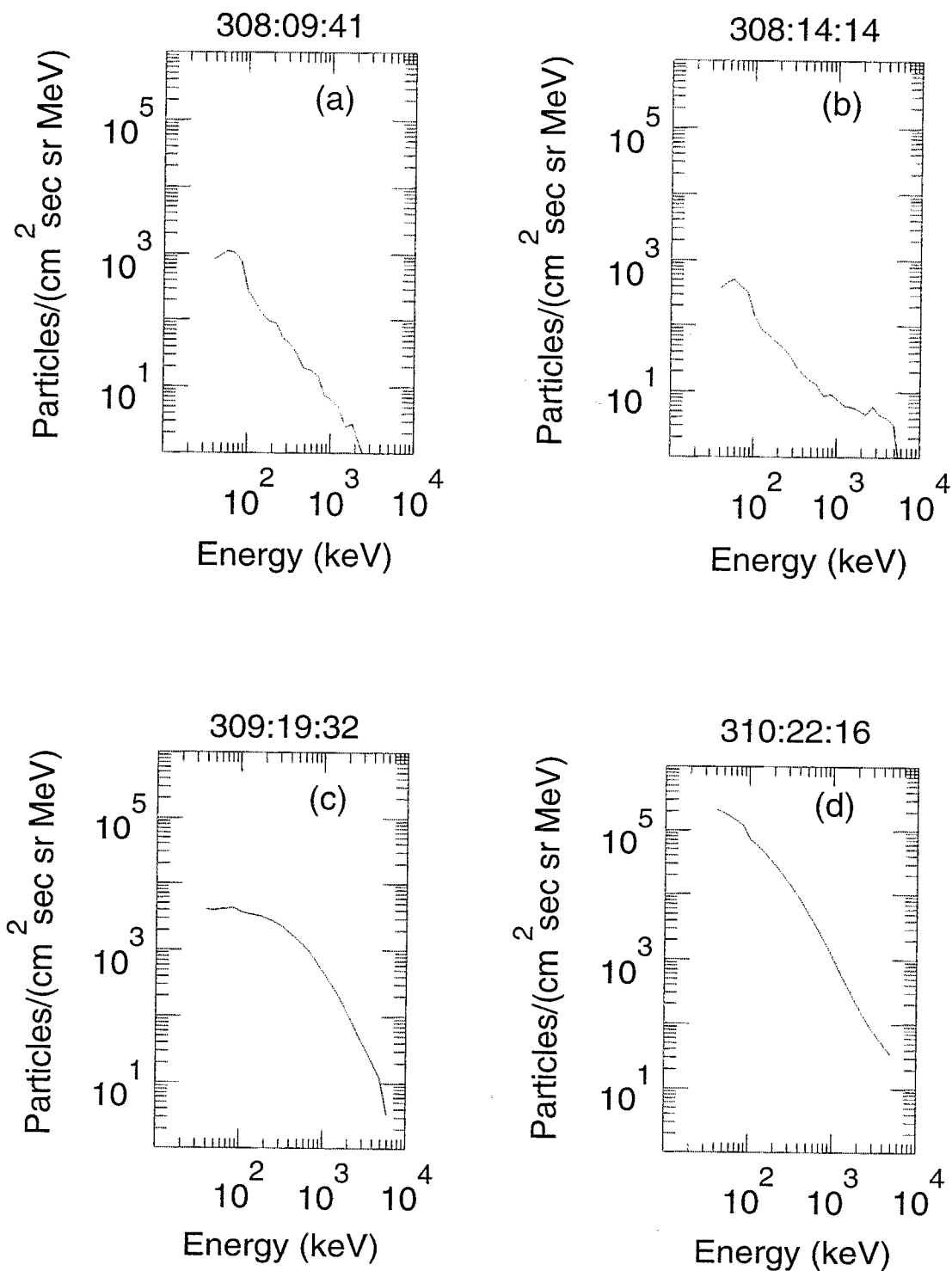


Figure 9. The 32 channel MFSA energy spectrum from the M detector (LEMS30 telescope) for four times following a large solar flare event in November 1997. In panel (d) note the large increase in the low-energy particles.

EPAM PHA Matrix

Start time = 1997 Day 311 06:00, End time = 1997 Day 311 18:00

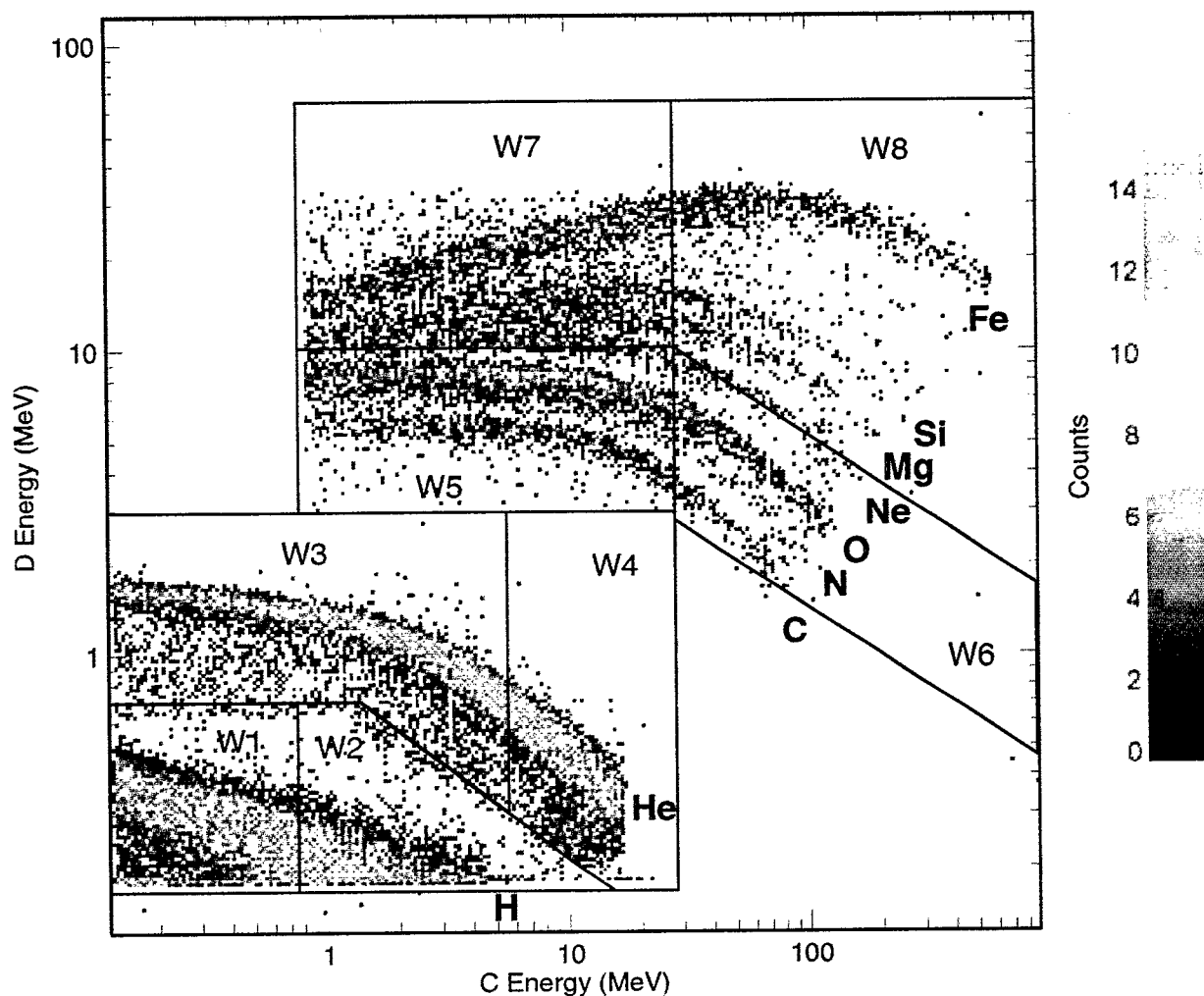


Figure 10. EPAM PHA matrix during the peak fluxes of the November 1997 solar flare event.

B. D. Williams and J. A. Krein provided thermal engineering. R. E. Thompson and J. A. Buttermore did all of the disassembly of HI-SCALE and assembly of the reconfigured instrument, EPAM.

References

- Chiu, M. C., von-Mehlem, U. I., Willey, C. E., Betenbaugh, T. M., Maynard, J. J., Krein, J. A., Conde, R. F., Gray, W. T., Hunt, Jr., J. W., Mosher, L. E., McCullough, M. G., Panneton, P. E., Staiger, J. P., and Rodberg, E. H.: 1998, 'ACE, Spacecraft'. *Space Sci. Rev.* **86**, 257.
- Lanzerotti, L. J., Armstrong, T. P., MacLennan, C. G., Simnett, G. M., Cheng, A. F., Gold, R. E., Thomson, D. J., Krimigis, S. M., Anderson, K. A., Hawkins, S. E., III, Pick, M., Roelof, E. C., Sarris, E. T., and Tappin, S. J.: 1993, 'Measurements of Hot Plasma in the Magnetosphere of Jupiter'. *Planetary Space Sci.* **41**, 893.
- Lanzerotti, L. J., Gold, R. E., Anderson, K. A., Armstrong, T. P., Lin, R. P., Krimigis, S. M., Pick, M., Roelof, E. C., Sarris, E. T., Simnett, G., and Frain, W. E.: 1983, in K.-P. Wenzel, R. G. Mars-

- den, and B. Battrock (eds.), 'The ISPM Experiment for Spectra, Composition, and Anisotropy Measurements of Charged Particles at Low Energies', *The International Solar Polar Mission — Its Scientific Investigations*, Noordwijk, The Netherlands, 141–154.
- Lanzerotti, L. J., Gold, R. E., Anderson, K. A., Armstrong, T. P., Lin, R. P., Krimigis, S. M., Pick, M., Roelof, E. C., Sarris, E. T., Simnett, G., and Frain, W. E.: 1992, 'Heliosphere Instrument for Spectra, Composition, and Anisotropy at Low Energies', *Astron. Astrophys.* **92**, 349.
- Zwickl, R. D., Doggett, K. A., Sahm, S., Barrett, W. P., Grubb, R. N., Detman, T. R., Raben, V. J., Smith, C. W., Riley, P., Gold, R. E., Mewaldt, R. A., and Maruyama, T.: 1998, 'The NOAA Real-Time Solar-Wind (RTSW) System Using ACE Data', *Space Sci. Rev.* **86**, 633.